

# Comprehensive scheme for subpixel variable block-size motion estimation

**Ying Zhang**

The Hong Kong Polytechnic University  
Department of Electronic and Information Engineering  
Hung Hom, Kowloon, Hong Kong  
and

Beijing Institute of Technology  
Department of Electronic Engineering  
Beijing 100081, China

**Wan-Chi Siu**

The Hong Kong Polytechnic University  
Department of Electronic and Information Engineering  
Hung Hom, Kowloon, Hong Kong

**Tingzhi Shen**

Beijing Institute of Technology  
Department of Electronic Engineering  
Beijing 100081, China

---

**Abstract.** *Fast variable block-size motion estimation is a key issue for real-time applications of the H.264, whereas the subpixel refinement takes up much computational time as compared to integer-pixel motion estimation. We propose a new fast subpixel precision variable block-size motion-estimation scheme. This algorithm uses the statistical information, which comes from the motion activities of the macroblocks (MBs) in the previous frame, to predict the characteristics of MBs in the current frame. Additionally, the distortion values and motion vectors of MBs in the previous frame are also considered as prior knowledge, based on which we can make decisions on early mode selection and early termination, and on whether or not to skip some candidate modes and candidate checking points. The intermediate results of subpixel motion estimation are used together with the prior knowledge to reduce subpixel search time when searching for stationary blocks. Our new directional information strategy is used in both integer-pixel motion estimation and subpixel motion estimation to accelerate the search procedure. Moreover, our algorithm can eliminate the subpixel motion estimation of all the unselected subpartition modes. The computational resources can then be spent on the modes and locations that deserve to be searched more than others. Extensive experimental is been done, the results of which show that the speed of our approach is nearly five times that of the fast algorithms in H.264 JM, with a better peak signal-to-noise ratio and better bit performance. © 2011 SPIE and IS&T. [DOI: 10.1117/1.3553438]*

---

## 1 Introduction

H.264 is an advanced video coding standard. Its high performance in coding is associated with its high computational

complexity. The standard supports seven modes of different block sizes for motion estimation (ME), which include the  $16 \times 16$  block size and its subpartitions. We did extensive work to analyze the statistics of the mode decision results. If quantization parameter (QP) is set to 28, >60% of the macroblocks (MBs) in many sequences are encoded as  $16 \times 16$  blocks after all modes are checked. A large amount of the computation did not provide a better result. This is illustrated in Sec. 2.1. These results shine some light on how we can accelerate variable block-size motion estimation. Although there are many fast ME algorithms in the literature, which are designed for the traditional ME structure with only one block size ( $16 \times 16$ ),<sup>1–9</sup> and there are some fast variable block-size ME algorithms.<sup>10–15</sup> Some fast variable block-size ME algorithms may check  $16 \times 16$  with  $8 \times 8$  first, then make early mode decision with the cost of  $16 \times 16$  and  $8 \times 8$  modes,<sup>16</sup> whereas in this paper, we propose to form an efficient variable block-size motion estimation algorithm that can make use of motion information and the relationship of the search results of different modes.

Subpixel refinement can greatly improve the performance of motion estimation both in terms of compression ratio and quality of the decoded image. However, the ratio between the time spent on fast integer-pixel search<sup>1–9</sup> and full position subpixel refinement (with partial distortion search strategy) could be nearly 1:6. The cost of this much computational time makes the subpixel refinement too costly. Some fast subpixel ME algorithms are available in the literature. One possible method is to perform an interpolation-free subpixel ME,<sup>17,18</sup> while another possible way is to do a candidate reduction subpixel ME,<sup>19,20</sup> and there are also some algorithms

---

Paper 10089R received Jun. 2, 2010; revised manuscript received Dec. 23, 2010; accepted for publication Jan. 18, 2011; published online Mar. 25, 2011.

1017-9909/2011/20(1)/013014/20/\$25.00 © 2011 SPIE and IS&T

that use the subpixel motion vector (MV) of large block sizes to predict the subpixel motion vector of small block sizes.<sup>21</sup> The interpolation-free subpixel ME algorithms use the ME cost of neighboring integer-pixel positions and a parabolic model to form the distortion surface of subpixel resolution positions, from which the best-match subpixel position can be found without image interpolation. In the candidate reduction subpixel ME algorithms, the ME cost of neighboring integer-pixel points is used to pick some subpixel positions as candidates, then, only these candidate subpixel positions will be checked. The accuracy of the interpolation-free subpixel ME is very close to a full position subpixel ME algorithm, but it still requires quite heavy computational time. On the other hand, the increase in bits of the candidate reduction subpixel ME algorithm is obvious, although its speed is faster. The computational complexity of Ref. 21 is between that of Refs. 19 and 20. However, although Ref. 21 can save some subpixel search computation for the partition modes, full position subpixel ME must generally be done for the  $16 \times 16$  block. The overall computational burden appears to be  $>16$  times more in terms of the SAD calculation. After careful observation, we find that the additional prior knowledge about the video sequence being coded can improve the search speed with little degradation on the search result. Also, the intermediate search results are extremely useful to speed up the estimation process of our algorithm.

In this paper, we design a new scheme making much better use of motion information as the prior knowledge so that the algorithm can achieve a more efficient performance and be adaptable to different sequences. The motion information includes distortion values, statistical distortion distribution, motion vectors, block classification of MBs, distribution of macroblocks for different classes in the previous frame, and intermediate integer-pixel and subpixel ME results in the current frame.

The rest of this paper is organized as follows: In Sec. 2, we show our analysis of the relationships of the ME results of different block sizes, mode decisions, subpixel MEs, and of checking points. Then, in Sec. 3, a comprehensive scheme trying to optimize the subpixel precision variable block-size ME is given. In Sec. 4, we illustrate the results of our experimental work, and in Sec. 5 we conclude the important points of this paper and make elaborate on our further work.

## 2 Analysis

### 2.1 Relationship of Motion-Estimation Results of Different Block Sizes

#### 2.1.1 Statistics of inter- and intramodes and computation analysis

The ME of H.264 supports four intermodes that correspond to block sizes of  $P16 \times 16$ ,  $P16 \times 8$ ,  $P8 \times 16$  and  $P8 \times 8$ . Each of the  $P8 \times 8$  blocks can be further subpartitioned into  $8 \times 4$ ,  $4 \times 8$ , and  $4 \times 4$  blocks. Besides the intermode, the H.264 also supports intramode coding for macroblocks in an intercoding slice, which means the encoder checks the intramodes after the best intermode is selected and then chooses the best mode from all these modes. Let us examine the distribution pattern of the intramode and four intermodes of some typical sequences. The QP used in this analysis is 28. These include 18 sequences: “clarie,” “akiyo,” “mother and daughter,” “hall,” “silent,” “highway,”

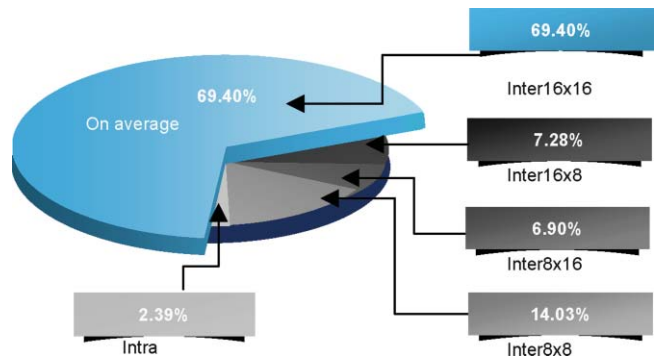


Fig. 1 Average distribution data of intra- and intermodes of all test sequences.

“container,” “erik,” “paris,” “foreman,” “football,” “waterfall,” “coastguard,” “bus,” “tempe,” “stefan,” “flower,” and “mobile.”

Figure 1 shows our experimental results, which are the averages of the distribution data of intra- and intermodes of all test sequences. As shown in the Fig. 1, the chance to choose a block type of  $P16 \times 16$ ,  $P16 \times 8$ ,  $P8 \times 16$ ,  $P8 \times 8$ , and Intra are 69.40, 7.28, 6.90, 14.03, and 2.39%, respectively.

#### 2.1.2 Motion vector prediction from other block mode sizes

General speaking, the motion vector can reflect the motion direction of a moving object in a video sequence; thus, the motion vectors of large block sizes should be helpful for motion searching on the small block sizes, especially for some close and related modes, such as  $16 \times 8$  mode is a close mode to  $16 \times 16$  mode. This fact is now being used in the ME module of H.264 reference software. The

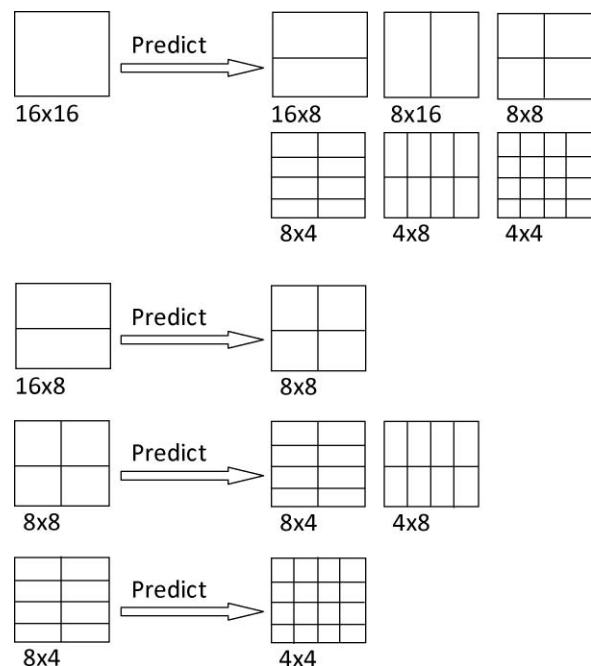


Fig. 2 Motion vector prediction of variable block size motion estimation.

**Table 1** Chance to choose  $P8 \times 8$  mode when a  $P16 \times 16$ ,  $P16 \times 8$ , or  $P8 \times 16$  mode is selected.

Sequences	P16 × 8 or P8 × 16 is selected in the first two stages and P8 × 8 is the best one after the third stage		P16 × 16 mode is selected in the first two stages and P8 × 8 is the best after the third stage	
Claire	49824	99%	325	1%
Akiyo	45641	99%	374	1%
Mother_				
Daughter	41670	99%	372	1%
Hall	43679	98%	885	2%
Silent	39636	99%	543	1%
Highway	40525	98%	673	2%
Container	45512	98%	827	2%
Erik	13001	97%	570	3%
Paris	35957	96%	1593	4%
Foreman	28342	96%	1329	4%
Football	14819	98%	366	2%
Waterfall	30835	97%	802	3%
Coastguard	22576	89%	2752	11%
Bus	22144	88%	3082	12%
Tempete	22541	85%	4092	15%
Stefan	26851	88%	3526	12%
Flower	28523	85%	5056	15%
Mobile	18708	72%	7187	28%
Average	31710	94%	1909	6%

method is that the motion vector of the  $16 \times 16$  mode is used as a predicted motion vector for all other modes; the motion vector of the  $16 \times 8$  mode is used as a predicted motion vector for the  $8 \times 8$  mode; the motion vector of the  $8 \times 8$  mode is used as a predicted motion vector for  $8 \times 4$  and  $4 \times 8$  modes; and the motion vector of the  $8 \times 4$  mode is used as a predicted motion vector for the  $4 \times 4$  mode, as shown in Fig. 2. This prediction strategy makes use of the relationship among motion vectors of different modes so that it could make the variable block-size ME algorithm more efficient. In order to accelerate the variable block-size ME further, we explored the relationship between mode decision results of the two stages of ME, and from this we have designed our mode prediction strategy.

### 2.1.3 Relationship between temporal best mode and final best mode in the mode decision

It is obvious that motion vectors of different block sizes are related to each other. The question is how to make use of this simple observation. In our algorithm, we use  $16 \times 16$

block size for the search in the first stage, then  $16 \times 8$  and  $8 \times 16$  block sizes, and  $8 \times 8$  block size and the other partitions in the third stage. If  $P16 \times 16$  is the best mode among  $P16 \times 16$ ,  $P16 \times 8$  and  $P8 \times 16$ , it means that a big block size is selected from among the three modes. This indicates that the moving object is probably not smaller than  $P16 \times 16$ , and the chance to choose a mode even smaller than  $P16 \times 8$  and  $P8 \times 16$  is low. If this assumption is true, then modes in the third stage can be skipped and the  $P16 \times 16$  mode can be selected as the best mode. We may then save a substantial amount of computation on  $8 \times 8$  mode and its subpartitions.

The results of our experimental work are shown in Table 1, which is divided into two columns. The first column shows the cases where a small block size has been selected in the first two stages ( $P16 \times 8$  or  $P8 \times 16$ ), and subsequently, a smaller block size ( $P8 \times 8$ ) is found to be better in the third stage. The first subcolumn gives the number of macroblocks, and the second subcolumn gives the percentage of macroblocks resulting from the respective conditions. The second column shows cases to the contrary,

where a large block size has been selected in the first two stages ( $P16 \times 16$ ), but after the third stage, a small block size ( $P8 \times 8$ ) is chosen as the best one among all inter-modes. Each of these two columns is divided into two sub-columns; one is the number of macroblocks in the corresponding cases, whereas the other is the percentage. (The QP used in this analysis was 28.) From the data in Table 1, we can see that, for most sequences, the intermediate mode decision results are usually consistent with the final mode decision results. Hence, we can make use of this fact to formulate our mode prediction strategy.

## 2.2 Relationship between Mode Decision and Subpixel Motion Estimation

### 2.2.1 Why do we need subpixel motion estimation?

There are many reasons why subpixel ME can enhance the performance of ME by eliminating the temporal redundancy, as follows:

1. Sampling: It is common that moving objects have a subpixel displacement between two frames. Because of the sampling effect, only the values of integer-pixel positions are available. Then in the ME procedure, after the integer-pixel search, a better match could be obtained by subpixel ME on the interpolated image.
2. Camera shaking: Camera shaking may bring motion effect to stationary objects. Hence, a stationary object may also have subpixel motion vectors.
3. Noise: Even a white wall can have subpixel motion, for example, when the noise generated by a camera is obvious, as we can see from the hall sequence.
4. Lighting conditions: The light on an object may change no matter whether the object is moving or stationary. In this case, the best match of the current block is probably to be found on a subpixel precision position because the light change may be slight.

According to our experimental results of 18 standard test sequences with QP = 28, the compression ratio and the peak signal-to-noise ratio (PSNR) of the decoded videos are 28 and 36.76 dB for the encoding process, using a ME algorithm with only integer-pixel search, whereas they are 50 and 37.01 dB for the encoding process with both integer-pixel search and subpixel refinement. Hence, subpixel refinement can greatly improve the performance of ME in terms of both compression ratio and decoded image quality.

### 2.2.2 Why do we need variable block-size motion estimation?

A moving object may spread among several MBs. On the other hand, in one MB there may be more than one object. If we perform ME with only a  $16 \times 16$  block size, then we may not find the best match for any of the objects in the block. To solve this problem involves H.264 variable block-size ME, which is a key feature of our investigation.

### 2.2.3 Mode decision not dependent on subpixel motion estimation

Ideally, mode decision is made after completion of integer-pixel ME and subpixel ME of all modes. This is time con-

**Table 2** Comparison of the results of making mode decision after (i) subpixel precision and (ii) integer pixel precision ME.

Sequences	Cases with the same results		Cases with different results	
Claire	52930	89.11%	6470	10.89%
Akiyo	52866	89.00%	6534	11.00%
Mother_				
Daughter	47183	79.43%	12217	20.57%
Hall	54008	90.92%	5392	9.08%
Silent	50600	85.19%	8800	14.81%
Highway	47871	80.59%	11529	19.41%
Container	47871	80.59%	11529	19.41%
Erik	15605	78.81%	4195	21.19%
Paris	47483	79.94%	11917	20.06%
Foreman	37288	62.77%	22112	37.23%
Football	25685	72.07%	9955	27.93%
Waterfall	34911	58.77%	24489	41.23%
Coastguard	29002	48.82%	30398	51.18%
Bus	28771	48.44%	30629	51.56%
Tempete	25172	42.38%	34228	57.62%
Stefan	30997	52.18%	28403	47.82%
Flower	34073	57.36%	25327	42.64%
Mobile	19627	33.04%	39773	66.96%
Average	37886	68.30%	17994	31.70%

suming. In order to save time, we may make mode decision after the completion of integer precision ME of all modes.

Table 2 gives our experimental results on this issue, which shows that subpixel ME does not change the result of the mode decision in most cases. Hence, even though the subpixel ME is an essential part for a precision ME, it can be done after the mode decision is made.

We have also inspected the relationship of the mode decision and subpixel ME from another point of view. This is to examine the bits spent on motion vectors, modes, and residual errors in the bit stream coded with (i) mode decision made after subpixel ME and (ii) mode decision made after integer-pixel ME. In both cases, both integer and subpixel ME were carried out. However, in case (ii) mode decision was made after making the integer-pixel ME of all possible modes, which saves much computation compared to case (i), because in this case, subpixel ME is only required to be carried out for the selected mode. Table 3 shows our experimental results, in which “MV bits” means bits spent on motion vector, “Mode bits” means bits spent on block mode, “Coeff bits” means bits spent on residual error, “Others bits” means bits spent on slice head,  $\delta$ -quantization parameter, and

**Table 3** Bits consumption for two mode decision strategies.

Sequences	(i) Mode decision made after Sub-pixel ME						(ii) Mode decision made after Integer-pixel ME					
	MV bits	Mode bits	Coeff bits	Others bits	Intra bits	Total bits	MV bits	Mode bits	Coeff bits	Others bits	Intrabits bits	Total bits
Claire	88230	63405	193766	52084	9019	406504	60094	84405	216792	57039	11302	429632
Akiyo	85724	67941	217374	50125	972	422136	48740	82189	268117	55380	5150	459576
Mother_Daughter	179890	102458	325079	84764	38825	731016	123518	126891	330210	89858	70523	741000
Hall	172608	116434	843605	122597	76732	1331976	62466	111051	745653	104729	147965	1171864
Silent	223052	112456	618936	92767	181197	1228408	114826	139109	495208	81900	294805	1125848
Highway	248594	112633	806937	103560	97396	1369120	164174	145919	756277	106702	287472	1460544
Container	85558	81533	705236	88857	23760	984944	51548	85781	821346	98591	28174	1085440
Erik	95772	50109	833894	54916	5741	1040432	49850	63236	745001	45743	34858	938688
Paris	367108	185073	2193839	152665	120307	3018992	135008	213310	1658155	116801	290406	2413680
Foreman	500578	211924	1066007	179814	152917	2111240	295248	278363	1020995	169276	337374	2101256
Football	313580	105909	1449200	126068	1442707	3437464	144824	113548	865210	96063	2127811	3347456
Waterfall	230474	168623	989743	182320	128	1571288	133568	172309	1110874	197381	1940	1616072
Coastguard	537904	283096	5928684	352159	147301	7249144	262040	275001	5215790	310374	890939	6954144
Bus	633878	296344	5483820	326551	248695	6989288	273570	295007	4445853	273872	1358394	6646696
Tempete	562084	306161	5969702	354073	360844	7552864	248672	292224	5626664	317481	704935	7189976
Stefan	590192	286837	5451709	313092	276418	6918248	233710	278903	4944901	268490	763084	6489088
Flower	513510	295837	8485125	286302	9578	9590352	206498	263659	8046880	252709	67718	8837464
Mobile	673562	381365	10679043	452908	6802	12193680	279508	398458	9403748	370456	347846	10800016
Average	339017	179341	2902317	187535	177741	3785950	160437	189965	2595426	167380	431705	3544913
Percent (%)	8.95	4.74	76.66	4.95	4.69		4.53	5.36	73.22	4.72	12.18	

“Intrabits” means bits spent on intrablocks in the intercoded frames.

It is interesting to note from Table 3 that although the mode decision was made after subpixel ME, case (i) requires lower MV bits (339,017 bits) and Mode bits (179,341 bits); yet case (ii) for which the Mode decision was made after integer-pixel ME only requires fewer Coeff bits (2,595,426 bits) than that in case (i) (2,902,317 bits). Consequently as an overall result, case (ii) requires fewer bits than case (i) on average. Hence, different from the conventional approach (such as that used in H.264 JM12.2), we prefer to make a mode decision after integer-pixel ME, which requires one to perform subpixel ME for only the best mode; hence, it reduces computational effort substantially.

### 2.3 Relationship among Candidate Checking Points of Half-Pixel Motion Estimation

Correlation is widely used to reveal the relationship among signals from different sources. Let us also make use of this mathematical tool and calculate the correlation coefficients

of half-pixel point pairs to reveal the relationship among them. Recall that the correlation coefficient,  $\rho_{X,Y}$ , between two random variables  $X$  and  $Y$  is defined as follows:

$$\rho_{X,Y} = \frac{\text{cov}(X, Y)}{\sigma_X \sigma_Y} = \frac{E[(X - \mu_x)(Y - \mu_y)]}{\sigma_X \sigma_Y}, \quad (1)$$

where  $\text{cov}(X,Y)$  means the covariance,  $\mu_x$  and  $\mu_y$  are the expected values,  $\sigma_x$  and  $\sigma_y$  are the standard deviations of  $X$  and  $Y$ .

In Fig. 3, integer-pixel locations are indicated by big circles, whereas half-pixel locations are indicated by small circles. Let us label eight nearby half-pixels of the best integer pixel 0 as half-pixel points 1, 2, ..., 7. Each half-pixel point of 0 can form seven pairs of half-pixels: Pair 1 to pair 7, with the rest of the half-pixel points, as indicated in Fig. 4.

In our experimental work, after the best integer location was found for each block, the correlation coefficients of its corresponding pairs—Pair 1 to pair 7—were calculated with Eq. (1). The values of these seven half-pixel correlation coefficients were added, respectively, to seven accumulators for

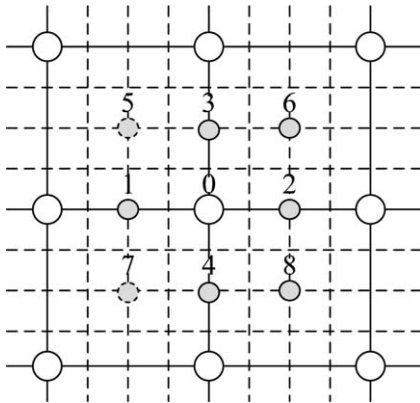


Fig. 3 Candidate positions of half-pixel ME.

all block locations and mode-type positions (including  $16 \times 16$ ,  $16 \times 8$ ,  $8 \times 16$ ,  $8 \times 8$ ,  $8 \times 4$ ,  $4 \times 8$ ,  $4 \times 4$ ). We accumulated the seven correlation coefficients of all blocks in 150 frames of each test sequence, respectively. The seven values shown in Fig. 5 are the average values of 18 sequences, in which the vertical axis indicates the accumulated values of the correlation coefficients and the horizontal axis indicates pair numbers. This statistical result shows that the accumulated values of correlation coefficients are consistent with the distance between the two points of a pair. That is, if the distance is shorter, it is more correlated. Hence, in our algorithm, the eight half-pixel points are grouped into near-neighbor points and far-neighbor points according to the distance between the half-pixel point and the best integer point.

Let us define that points 1–4 are near neighbors because they are closer to the best integer-pixel position compared to points 5–8, which are far neighbors. Each far neighbor point is on the perpendicular bisector of two near-neighbor points. The search results of the far-neighbor points are supposed to be related to that of the near-neighbor points. Further experimental work was done to check whether the risk of missing the best match point is worth taking, and its results are shown in Table 4.

We trust that the idea of directional tendency will work for subpixel ME, which is only to make necessary tests on

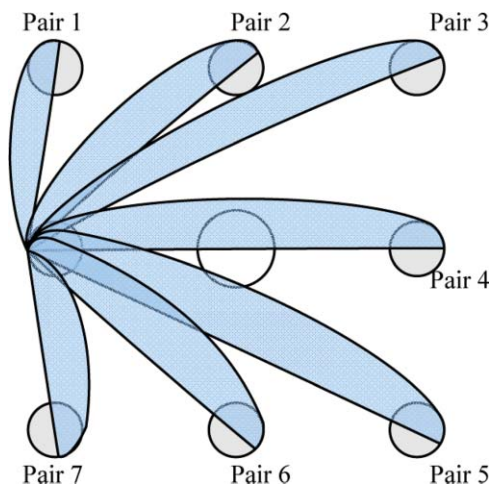


Fig. 4 Definition of point pairs for correlation coefficient calculation.

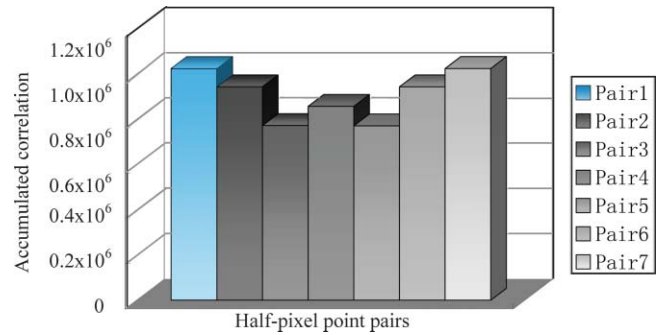


Fig. 5 Cross-correlation of seven point pairs.

locations along the direction indicated by the search path, and this idea should work even better than that for integer-pixel ME.<sup>7</sup>

We have verified this idea with the following experimental work in order to avoid the risk missing important locations. We checked the four near neighbors, collected the results, and then checked the four far neighbors and counted the

Table 4 Risk of missing the best match point.

Sequences	Total number of half-pixel MEs	Number of contradictions	Rate (%) [(3)/(2)]
Column (1)	(2)	(3)	(4)
Claire	59004	414	0.70
Akiyo	59004	379	0.64
Mother_			
Daughter	59004	1040	1.76
Hall	59004	212	0.36
Silent	59004	453	0.77
Highway	59004	915	1.55
Container	59004	164	0.28
Erik	19404	294	1.52
Paris	59004	370	0.63
Foreman	59004	2850	4.83
Football	35244	998	2.83
Waterfall	59004	235	0.40
Coastguard	59004	226	0.38
Bus	59004	355	0.60
Tempete	59004	630	1.07
Stefan	59004	321	0.54
Flower	59004	442	0.75
Mobile	59004	615	1.04
Average	55484	606	1.15

number of half-pixel ME operations required in a counter, counter1. If the best near-neighbor point was 3 for example, and the best far-neighbor point was 7 or 8, we increased the number of contradictions in another counter, counter2. This gives the number of times we got a half-pixel motion vector, which has an opposite direction to the search result of near neighbors. The total number of half-pixel ME and the number of contradictions are shown in columns (2) and (3), respectively, of Table 4. The ratio between columns (3) and (2) is shown in column (4), which indicates that the directional information obtained from the search result of near-neighbor points is reliable.

#### 2.4 Relationship between Half- and Quarter-Pixel Motion-Estimation Results

Half-pixel ME and quarter-pixel ME are usually used to refine the integer-pixel ME result. Half-pixel refinement is conducted on neighbor points surrounding the best integer-pixel point. The best half-pixel point will then be the center for quarter-pixel refinement, which may not be the original center point of half-pixel refinement. Hence, the quarter-pixel motion vector should not be predicted from only a half-pixel motion vector.

It is found<sup>7,8</sup> that block classification is an effective way to determine whether or not a macroblock belongs to the same moving object as its neighboring MBs. It provides a noticeable improvement in the integer-pixel ME algorithm. Is it possible to combine the block-classification result of the previous frame and the half-pixel ME result to make an early termination before the quarter-pixel ME?

According to the block classification, we can predetermine the current MB as an ordinary block or a special block. If we predetermine it as an ordinary block, then it indicates that the current MB probably belongs to the same moving object as its neighboring MBs. The blocks that belong to the same moving object should have similar or even the same motion vector. The motion of a moving object within a small set of consecutive frames should be consistent. Hence, we suppose if the current block is part of a predetermined ordinary macroblock, then its collocated macroblock has a zero motion vector, and the motion vector of the current block after half-pixel refinement is also zero. The current block is then most likely to be a stationary block, and it will also get a zero motion vector after quarter-pixel refinement.

In our experimental work, we calculated the chances of getting a zero vector or nonzero vector after a quarter-pixel refinement when the condition to predict the current block as a stationary block is true. The results of our experimental work listed in Table 5 verify that our assumption is true, which means that the chance of missing a valid quarter-pixel motion vector is usually not high.

### 3 Algorithm Development

#### 3.1 Motion Information for Early Termination and Early Mode Decision

##### 3.1.1 Block classification according to variable block size motion information

Our block classification is designed to imply the motion characteristic of macroblocks so that we can apply fast strategies to macroblocks (and their subpartition blocks) with certain features. As a recent practice, during the ME procedure for

only  $16 \times 16$  blocks, the motion vectors of neighboring MBs were used to predict the motion vector of the current MB before the pattern search stage. Then, the pattern search starts from the point indicated by the best-predicted motion vector. After the pattern search stage, if the final motion vector is not the same as the best-predicted motion vector, then the macroblock may contain a different moving object from its neighboring MBs; thus, we classify it to fall into the special macroblock group (group S), whereas the other macroblocks (with the same MV) are classified into the ordinary macroblock group (group O). In this scheme, for ME with variable block sizes, we have seven groups of “the best” predicted motion vectors corresponding to seven block sizes. Among the best-predicted motion vectors of the seven partitions, only those of the best mode are used in the block-classification process. If the best mode is classified as belonging to the special block group, then the current macroblock is set as a special MB. Whether it is a “special MB” and an “ordinary MB” of a MB in the current frame can be “predetermined” according to the block classification of the previous frame. For a special MB in the previous frame, its collocated MB and its eight surrounding MBs are predetermined as special MBs, and others are predetermined as ordinary MBs in the current frame. Hence, the classification method works well in the variable block-size ME scheme.

##### 3.1.2 Distribution of best mode SAD values of macroblocks in successive frames

Motion continuity exists not only on neighboring areas in one frame but also among successive frames. If the sum-of-absolute-differences (SAD) statistics of successive frames are similar to each other, then the statistical distribution of SADs of the current frame can be predicted by the SAD statistics of the previous frame. This appears true for ME with  $16 \times 16$  blocks. For variable block-size ME, can we find a similar correlation? The SAD of a macroblock in variable block-size ME is composed of the SAD of each block in the current macroblock and its corresponding best match block in the reference frame. In Fig. 6, SAD represents the

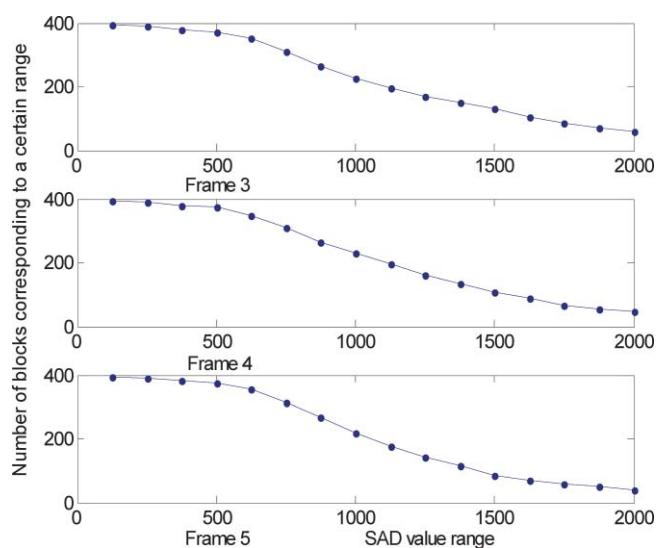


Fig. 6 Number of blocks corresponding to a certain range of SAD.

**Table 5** Chance to ignore an existing quarter-pixel MV.

Sequences	Number of predicted stationary blocks	Predicted as a stationary block, and the subpixel MV is still zero after QPEL refinement	(4) Rate (%) [(3)/(2)]	Predicted as a stationary block, but the subpixel MV becomes nonzero after QPEL refinement	(6) Rate (%) [(5)/(2)]
Column (1)	(2)	(3)		(5)	(6)
Claire	42095	37322	88.66	4773	11.34
Akiyo	43273	34193	79.02	9080	20.98
Mother_					
Daughter	28787	23047	80.06	5740	19.94
Hall	43604	35061	80.41	8543	19.59
Silent	36248	31261	86.24	4987	13.76
Highway	13887	11002	79.23	2885	20.77
Container	36543	30291	82.89	6252	17.11
Erik	11446	9793	85.56	1653	14.44
Paris	32701	28691	87.74	4010	12.26
Foreman	2078	1598	76.90	480	23.10
Football	2626	1486	56.59	1140	43.41
Waterfall	5017	2364	47.12	2653	52.88
Coastguard	679	258	38.00	421	62.00
Bus	1224	985	80.47	239	19.53
Tempete	4602	2602	56.54	2000	43.46
Stefan	3532	2280	64.55	1252	35.45
Flower	12751	11492	90.13	1259	9.87
Mobile	1001	420	41.96	581	58.04
Average	17894	14675	72.34	3219	27.66

SAD values of the best mode of each of the macroblocks in frames 3–5 of the foreman sequence. Because most of the SAD values of these frames are distributed within the range 0–2000, only SAD values in this range are shown in Fig. 6 for illustration. These values are divided into 16 groups (bins). The numbers of macroblocks having SAD values larger than the minimum values of groups are plotted on the graph by dots. In Fig. 6, it is clear that the SAD statistics of the three frames are similar to each other. We have found similar patterns on other consecutive frames making use of this analysis with other test sequences (such as hall and football video sequences), with slow and fast motion activities.

Hence, we can make a prediction on the statistical SAD distribution of the current frame from that of the previous frame. The method is to let the SAD statistics of the previous

frame be the predicted SAD statistics of the current frame before ME and update it with the real SAD statistics of the current frame after ME.

The predicted SAD statistics of the current frame can help us to find an effective threshold to be used in the next frame. After checking all the predicted motion vectors, we may compare the SAD value of the best-predicted motion vector to the threshold to make a decision on the early termination of one mode. This strategy makes it possible for us to skip further searching for some predetermined ordinary macroblocks after the motion vector prediction. This is the same approach as the one for which we can do for ME with  $16 \times 16$  blocks. It can also have a good effect on the variable block-size ME because this allows us to choose early termination before the pattern search of each mode. In this way, we can reduce the computation time spent on pattern search. If



the pattern search is skipped, then the final MV of the block will be the same as its best-predicted MV. Subsequently, the block will become an ordinary block after ME of the current frame. It means early termination generates more ordinary MBs. It is necessary to control the number of blocks chosen for early termination in order to maintain the performance of the ME algorithm. Hence, we need to control the threshold for early termination. From experimental work, we note that the number of ordinary MBs of the successive frames do not change much. Thus, we expect that the number of ordinary MBs in the current frame be similar to that of the previous frame.

Experimental evidence shows us that the number of ordinary macroblocks in the current frame is closely related to the threshold for early termination. The threshold can be obtained according to the predicted number of ordinary MBs of the current frame. Hence, in our design we find the threshold for early termination by looking up the SAD value-number distribution graph of macroblocks (as shown in Fig. 6) of the previous frame, which is a prediction of the current frame. The SAD value corresponding to the number of ordinary macroblocks in the previous frame is taken as the threshold required.

In this example, we divided the range into 16 groups. If the threshold is too low, then this fast strategy may not work. Furthermore, an unexpectedly higher threshold could compromise too much the precision of the search. Hence, we suggest an upper bound and lower bound for the threshold, which are 800 and 1500, respectively, according to the results of a large number of experiments. The block classification and threshold calculation have been designed in such a way that they are suitable for variable block-size ME.

### 3.2 Eliminating Subpixel Motion Estimation of All Unselected Modes

Because mode decisions do not depend on the subpixel ME, we can consider them as two separate problems and deal with them individually. This means that we can perform integer-pixel ME for each mode, choose the best mode according to their rate distortion values, and then perform subpixel ME for only the best mode from the point given by the motion vector of the best integer mode, as shown in Fig. 7.

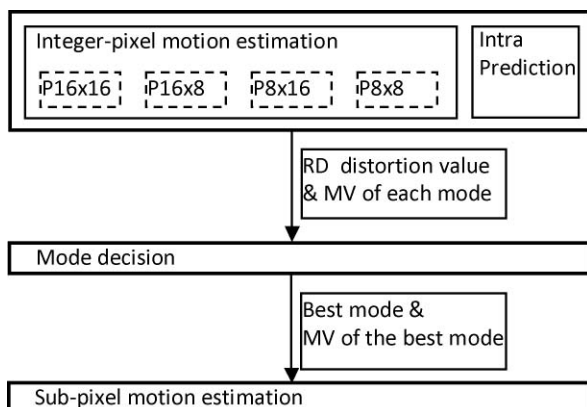


Fig. 7 Process of integer-pixel & sub-pixel motion estimation.

### 3.3 Fast Subpixel Strategies of One Mode

#### 3.3.1 Directional search strategy for subpixel motion estimation

Let us use the analysis results in Sec. 2.3 to accelerate the full-position subpixel ME algorithm. The full-position subpixel ME with early termination strategy has been used in the JM model of H.264. It contains two consecutive steps: half-pixel refinement and quarter-pixel refinement. Half-pixel refinement needs to examine all eight half-pixel checking points surrounding the best integer point, and the quarter-pixel refinement needs to examine eight quarter-pixel checking points surrounding the best half-pixel point. It must calculate the SAD of subpixel positions 16 times. According to our experimental work the additional time required by this algorithm is nearly six times that of the time spent on our fast integer-pixel search procedure.

The relationship among candidate positions of the half-pixel ME shows that we can rely on the directional information obtained from the search result of near-neighbor points to skip some of the far-neighbor points before we examine them (see Sec. 2.3). Let us refer to Fig. 3 for our fast half-pixel ME process. There are eight half-pixel points surrounding the integer pixel 0 (i.e., points 1–8).

Step 1: We need to examine the four near-neighbor points surrounding the best integer-pixel point, 1–4. Let us keep the motion vector and minimum SAD value of the best point as the temporal half-pixel ME result.

Step 2: If one of the four near-neighbor points is better than the best integer-pixel point, we examine the two far-neighbor points besides the best near-neighbor point. For example, if the best near-neighbor point is point 2, then points 6 and 8 will be examined. If a smaller SAD is found, then it will be stored as the minimum SAD and the motion of this point (i.e., the displacement between the best integer-pixel point and this point) will be set as the half-pixel ME result. Otherwise, we set the temporal result in step 1 as the half-pixel ME result.

Note that the two points encircled with a dashed line will not be examined in this fast refinement. This candidate rejection strategy is also applied to quarter-pixel refinement in our algorithm.

#### 3.3.2 Stationary block identification with the result of half-pixel motion estimation; and skipping quarter-pixel motion estimation for stationary blocks

In this part, the relationship between half- and quarter-pixel ME results will be combined with the prior knowledge of MBs in the previous frame to form a stationary block-identification strategy to skip the quarter-pixel ME for the stationary blocks. This is to accelerate further the subpixel ME algorithm.

If we find that the current block is a part of a predetermined ordinary MB and the motion vector of its co-located MB in the previous frame is a zero vector, then we may assume that the current block belongs to the same stationary object as its neighboring MBs. If the motion vector of the current block is a zero vector after half-pixel refinement (i.e., the condition for stationary block identification is true.), then it is more likely that the current block will have a zero motion vector after quarter-pixel refinement. Hence, we can consider skipping the quarter-pixel refinement of the current block.

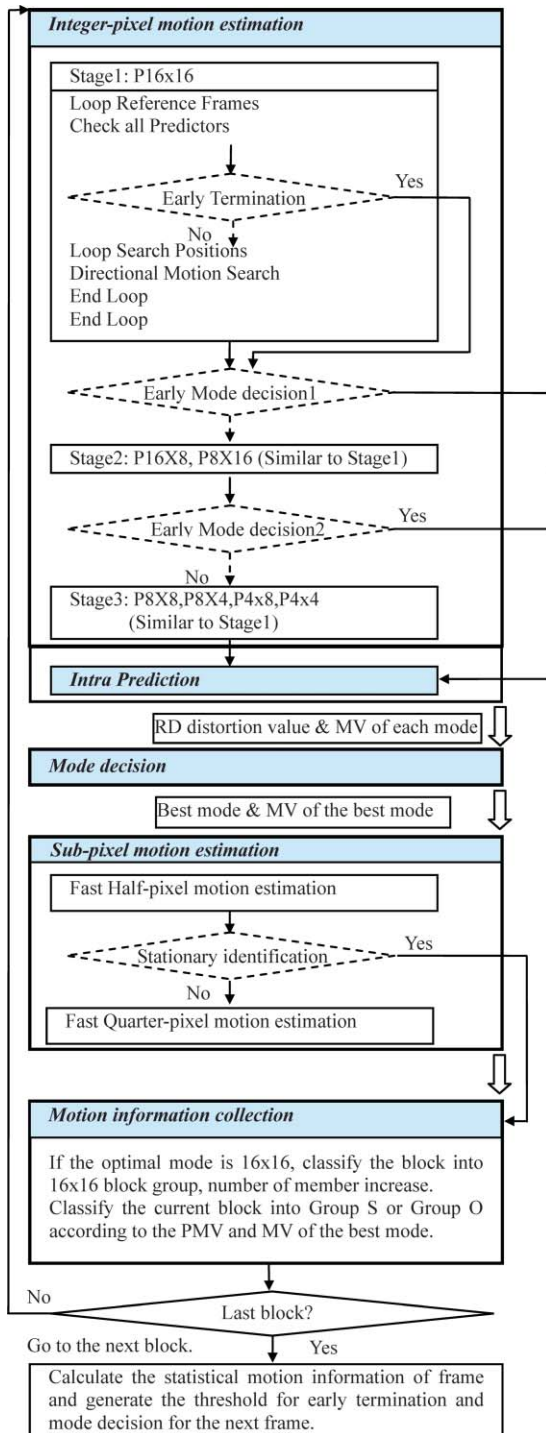


Fig. 8 Flowchart of the suggested algorithm.

### 3.4 Overall Structure of the Algorithm

Figure 8 shows a flowchart of the proposed approach. There are five major modules of operations in the structure, which are integer-pixel ME, intraprediction, mode decision, sub-pixel ME, and motion-information collection. The integer-pixel ME includes motion search for variable block sizes. The first stage of module one is to search for the  $16 \times 16$  block size; then in the second stage, the macroblock is divided into  $16 \times 8$  or  $8 \times 16$  blocks to carry out a motion

search on the small blocks, individually. In the third stage, the macroblock is further divided into  $8 \times 8$ ,  $8 \times 4$ ,  $4 \times 8$ , and  $4 \times 4$  blocks. After checking the intermodes, the intraprediction is then considered. There is one conditional execution for “early termination” in each stage (not shown on Fig. 8 for stages 2 and 3). And there are “early mode decision1” and “early mode decision2” after stage1 and stage2, respectively. The early termination check is carried out after checking all predictors that are motion vectors of the neighboring MBs in the spatial and temporal domains.

#### 3.4.1 Condition for early termination

The conditions for early termination are as follows:

1. The current MB is a predetermined ordinary macroblock.
2. The current minimum SAD for the macroblock is smaller than the threshold for early termination, which is calculated at the end of the ME of the last frame.
3. The current minimum SAD for the macroblock is smaller than the minimum SAD of the collocated MB.

Note that if the current block is a subpartition of a MB, then we will then scale the threshold value appropriate to the size of the current block. For example, if the current block is an  $8 \times 8$  block, the original threshold is 800. We then have to compare the current SAD with  $(800 * 8 * 8) / (16 * 16) = 200$  to make the decision for early termination. The scale factor will also be used for this block to form an appropriate threshold to assist fast mode decisions.

If the conditions are true, early termination will become effective, which means the best predicted motion vector (PMV) is selected as the final MV of the current block. The pattern search part is then skipped for this mode, and the ME process will move onto another mode with similar or smaller block sizes.

#### 3.4.2 Condition for early mode decision

The conditions for “early mode decision1” are as follows:

1. The current MB is a predetermined ordinary macroblock.
2. The current minimum SAD cost for the macroblock is smaller than the threshold for early termination, which is also used as the threshold for early termination.

Hence, if early mode decision1 is selected,  $16 \times 16$  is set to the best mode of the current MB and all the other modes are skipped. Otherwise, we will check  $16 \times 8$  and  $8 \times 16$  modes in stage 2.

At the end of stage 2, if we find that  $16 \times 16$  is the best mode among  $16 \times 16$ ,  $16 \times 8$  and  $8 \times 16$ , this forms the condition for early mode decision2. If this condition is true, then  $16 \times 16$  is selected as the best mode and  $8 \times 8$  and its subpartition block sizes are not considered.

After all inter- and intramodes are checked, the best mode will be selected in the mode decision module. If the intermode is selected, the subpixel ME is then carried out on the selected best mode.

There is also a chance for early termination (not shown in Fig. 8) after the half-pixel ME process in the subpixel

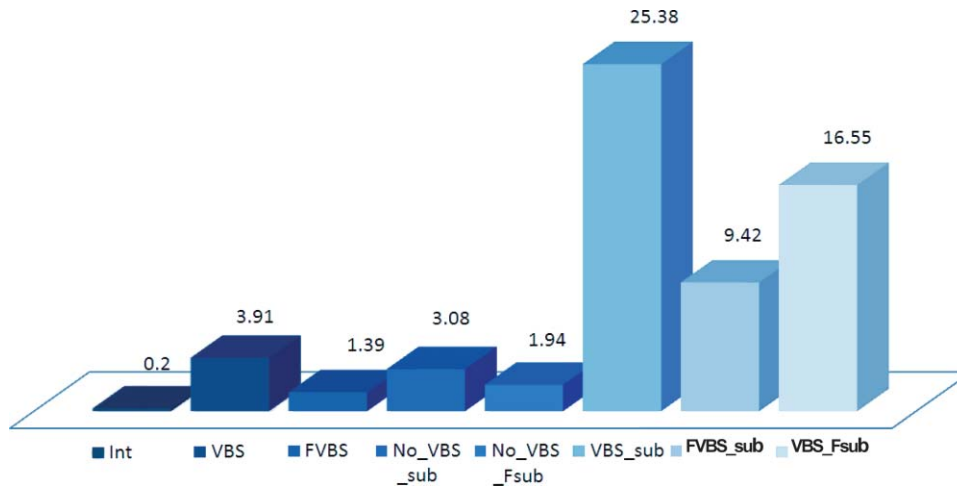


Fig. 9 ME time (in seconds) of various compositions of our fast strategies.

motion-estimation module. The conditions for this early termination are as follows:

1. The current MB is a predetermined ordinary macroblock.
2. The motion vector of the collocated MB is zero.
3. The motion vector of the current block with half-pixel refinement is zero.

The subpixel ME may be done on a subpartition mode of a  $P16 \times 16$  macroblock because the best mode can be any one of the four modes. Moreover, the fast directional approach can be used no matter whether the subpixel ME is conducted on an MB or a block.

The search process is then completed for a macroblock at this stage. In the next module, the motion information of the MB is calculated and stored to form the statistical motion information of the current frame, which will be used as prior knowledge to guide the ME procedure of the next frame. If the PMV of the current MB is equal to its final MV in the best mode, then the current macroblock is classified into the ordinary MB group and the number of ordinary MBs increases by 1. Then, the minimum SAD value of the MB is recorded. If an MB with its best possible mode consists of several blocks, then the SAD values of these blocks are used to form the SAD of this MB, possibly with the minimum value.

If all MBs have been processed, then the statistical motion information of the frame is obtained, and thresholds for early termination and the early mode decision for the next frame will be generated from the result of the statistics. The SAD values of all MBs are examined. The range of these SAD values is divided into 16 parts according to their values. Subsequently, as shown in Sec. 3.1.2, a new SAD value–number distribution is formed, which can be used to find the threshold for early termination by looking for the SAD value corresponding to the number of ordinary MBs of this frame. This is stored inside “the motion-information collection module” to be used in the next frame.

Note that both integer-pixel motion search and subpixel motion search processes of the algorithm make use of directional motion search. Further details of the directional integer-pixel ME is illustrated in Ref. 7, whereas the

directional subpixel ME method is given in Sec. 3.3.1 of this paper.

#### 4 Experimental Results

This fast subpixel precision variable block-size ME algorithm consists of three groups of fast strategies: a fast variable block-size ME strategy, an effective way to eliminate subpixel ME of all unselected modes; and a fast subpixel ME strategy. In this section, we will illustrate the results of our experimental work. We will initially make an analysis and verify the improvement of these three groups of our fast strategies independently. We then compare the performance of our fast variable block-size and subpixel ME strategies to existing algorithms, and show the overall performance of our work compared to other algorithms in the literature.

The software was the JM12.2 encoder. The proposed algorithm is combined with the mode selection procedure of the H.264 reference software (JM12.2) to improve the speed of ME so as to enhance the efficiency of the encoder. We used an IBM Notebook with Inter Core 2 Duo CPU T7300 2.0G and 2-gigabytes of RAM. The ME search range was 32. The QP was set to 28. The RDO optimization option was set to 1, which is the high complexity mode.

There were 18 test sequences with the common image format (CIF) used in our experimental work. Only the average values of the computation time (in seconds) of the experimental results are given as shown in Fig. 9. The abbreviations of this graph are as follows: “Int” stands for our fast integer-pixel ME;<sup>7</sup> VBS is variable block-size ME; “sub” is subpixel ME; “No” means the function is not used [e.g., “No\_VBS\_sub” means subpixel precision ME without variable block-size function, and this implies that it supports  $16 \times 16$  block size only (without using VBS)], and F represents that our fast strategies of the function were used (e.g., “FVBS\_sub” means fast variable block-size ME with subpixel refinement on each mode).

The y-axis of the graph shows the ME time in second. The number on the top of each block gives the average ME time for each scheme. We use four matrices in the form of ratios to make an analysis and to reflect the accuracy of our measurements,

**Table 6** Performance comparison of variable block-size ME algorithms.

Sequences	FS			EPZS			FORMER			PRES variable block size ME (integer PEL)		
	PSNR	Bits per pixel	Speedup (real time)	PSNR	Bits per pixel	Speedup (real time)	PSNR	Bits per pixel	Speedup (real time)	PSNR	Bits per pixel	Speedup (real time)
Claire	41.45	0.0475	1	41.36	0.0475	27	41.29	0.0445	84	41.29	0.0483	137
Akiyo	39.43	0.0546	1	39.40	0.0547	28	39.32	0.0467	140	39.35	0.0557	160
Mother_												
daughter	38.44	0.0748	1	38.42	0.0754	34	38.36	0.0675	76	38.38	0.0770	204
Hall	37.71	0.0994	1	37.68	0.0997	33	37.66	0.0825	115	37.67	0.1011	251
Silent	36.02	0.1138	1	36.02	0.1148	39	36.01	0.1069	97	36.02	0.1174	300
Highway	38.58	0.1207	1	38.54	0.1247	36	38.50	0.1214	67	38.57	0.1368	172
Container	36.06	0.1523	1	36.03	0.1526	45	36.01	0.1422	108	36.01	0.1536	362
Erik	37.15	0.1188	1	37.15	0.1193	32	37.15	0.1188	68	37.13	0.1211	222
Paris	35.87	0.2892	1	35.84	0.2896	36	35.82	0.2794	74	35.82	0.2961	205
Foreman	36.76	0.2337	1	36.74	0.2386	33	36.71	0.2321	40	36.68	0.2487	151
Football	37.54	0.2522	1	37.54	0.2561	40	37.52	0.2526	45	37.57	0.2605	136
Waterfall	34.27	0.3509	1	34.24	0.3508	48	34.16	0.3090	69	34.2	0.3523	266
Coastguard	34.94	0.6669	1	34.94	0.6692	46	34.93	0.6667	51	34.93	0.6706	236
Bus	35.24	0.8070	1	35.25	0.8150	46	35.25	0.8138	44	35.25	0.8252	203
Tempete	35.44	0.9194	1	35.42	0.9233	44	35.42	0.9171	44	35.39	0.9372	309
Stefan	36.01	0.8246	1	35.99	0.8274	43	35.99	0.8199	42	35.98	0.8339	237
Flower	36.16	1.0272	1	36.15	1.0288	44	36.12	1.0269	47	36.13	1.0331	266
Mobile	35.21	1.4225	1	35.19	1.4310	46	35.16	1.4294	47	35.18	1.4559	240
Average	36.79	0.4209	1	36.77	0.4233	40	36.74	0.4154	57	36.75	0.4292	219

$$r_1 = \frac{\text{MTime}(\text{FVBS\_sub})}{\text{MTime}(\text{VBS\_sub})} = \frac{9.42 \text{ s}}{25.38 \text{ s}} = 0.3712, \quad (2)$$

$$r_2 = \frac{\text{MTime}(\text{FVBS})}{\text{MTime}(\text{VBS})} = \frac{X_1 \text{ s}}{3.91 \text{ s}} \approx 0.3712. \quad (3)$$

The numerical values in Eqs. (2) and (3) are obtained from Fig. 9.  $r_1$  is the ratio between the motion estimation time of subpixel precision fast variable block-size ME and the ME time of the subpixel precision variable block-size ME without any fast mode decision strategy.  $r_2$  is the ratio between ME times of integer-pixel precision fast variable block-size ME algorithm and integer-pixel precision variable block-size ME without a fast mode decision strategy. These two ratios should be similar if we assume both VBS and subpixel ME depend on the resultant modes of a frame. From the Fig. 9, the ME time of subpixel precision fast variable block-size ME is 9.42 s and the ME time of subpixel precision original variable block-size ME is 25.38 s. Hence,  $r_1$  is obtained, which can be used to approximate the value of  $r_2$  as shown in

Eq. (3). Subsequently, the ME time of the integer-pixel precision fast variable block-size motion estimation,  $X_1$  can be estimated using Eq. (2). This gives  $r_2$ , which is  $3.91 \text{ s} \times 0.3712 = 1.45 \text{ s}$ . From Fig. 8, the ME time of integer-pixel precision fast variable block-size ME is 1.39 s. The estimated value is very close to this measured result, which means that our analysis is accurate and able to reveal the relation between the computational complexity of our algorithm with the fast mode decision method and that of the original algorithm without using the fast mode decision method.

Let us define the third and fourth ratios,

$$\begin{aligned} r_3 &= \frac{\text{MTime}(\text{VBS\_Fsub\_only})}{\text{MTime}(\text{VBS\_sub\_only})} \\ &= \frac{\text{MTime}(\text{VBS\_Fsub}) - \text{MTime}(\text{VBS})}{\text{MTime}(\text{VBS\_sub}) - \text{MTime}(\text{VBS})} \\ &= \frac{16.55 - 3.91 \text{ s}}{25.38 - 3.91 \text{ s}} = \frac{12.64 \text{ s}}{21.47 \text{ s}} = 0.5887, \end{aligned} \quad (4)$$

**Table 7** Performance comparison of subpixel ME algorithms (with fixed block size:  $16 \times 16$ ).

Sequences	Full Position subpixel ME (QPEL)			Present subpixel ME (QPEL)			Interpolation-free subpixel ME (QPEL) <sup>a</sup>			Fast Fractional PEL subpixel ME (QPEL) <sup>b</sup>		
	PSNR	Bits per pixel	Speedup (real time)	PSNR	Bits per pixel	Speedup (real time)	PSNR	Bits per pixel	Speedup (real time)	PSNR	Bits per pixel	Speedup (real time)
Claire	41.57	0.0320	1	41.59	0.0327	2.54	41.57	0.0320	1.49	41.56	0.0366	2.34
Akiyo	39.75	0.0344	1	39.73	0.0360	1.92	39.71	0.0345	1.36	39.68	0.0395	1.92
Mother_												
daughter	38.89	0.0562	1	38.87	0.0563	1.96	38.85	0.0563	0.89	38.83	0.0597	2.37
Hall	37.82	0.1011	1	37.80	0.1000	2.15	37.81	0.1003	1.03	37.79	0.1030	2.31
Silent	36.11	0.1005	1	36.11	0.1007	2.19	36.10	0.1008	1.23	36.10	0.1061	2.62
Highway	38.52	0.1063	1	38.53	0.1057	1.89	38.55	0.1058	1.19	38.53	0.1155	2.70
Container	35.99	0.0751	1	36.00	0.0784	2.25	35.99	0.0751	1.06	36.05	0.0897	2.88
Erik	37.08	0.0843	1	37.08	0.0847	2.28	37.07	0.0844	1.13	37.02	0.0925	2.93
Paris	35.92	0.2484	1	35.90	0.2497	1.66	35.91	0.2484	0.97	35.89	0.2659	2.13
Foreman	36.89	0.1783	1	36.91	0.1818	1.22	36.91	0.1802	1.13	36.85	0.1995	2.22
Football	37.78	0.2497	1	37.77	0.2495	1.40	37.75	0.2511	1.41	37.70	0.2550	2.25
Waterfall	34.98	0.1311	1	35.00	0.1304	1.47	34.98	0.1308	0.83	35.03	0.1466	2.35
Coastguard	35.22	0.5154	1	35.22	0.5156	1.25	35.20	0.5157	1.15	35.11	0.5596	2.00
Bus	35.56	0.5306	1	35.57	0.5316	1.38	35.56	0.5316	1.49	35.45	0.5939	2.14
Tempete	35.37	0.5379	1	35.35	0.5437	1.50	35.37	0.5369	1.36	35.26	0.6220	2.66
Stefan	36.25	0.5152	1	36.25	0.5181	1.37	36.24	0.5152	0.89	36.04	0.5840	2.57
Flower	36.04	0.7096	1	36.05	0.7107	1.48	36.05	0.7106	1.03	36.04	0.7833	2.71
Mobile	34.97	0.8701	1	34.95	0.8764	1.13	34.96	0.8722	1.23	34.80	1.0147	1.85
Average	36.93	0.2820	1	36.93	0.2835	1.62	36.92	0.2823	1.19	36.87	0.3148	2.35
$\Delta$ ,%, speedup				0	0.53% $\uparrow$	1.62	0.01 $\downarrow$	0.11% $\uparrow$	1.19	0.05 $\downarrow$	11.63% $\uparrow$	2.35

<sup>a</sup>Reference 16.<sup>b</sup>Reference 19.

$$\begin{aligned}
r_4 &= \frac{\text{METime}(\text{No\_VBS\_Fsub\_only})}{\text{METime}(\text{No\_VBS\_sub\_only})} \\
&= \frac{\text{METime}(\text{No\_VBS\_Fsub}) - \text{METime}(\text{Int})}{\text{METime}(\text{No\_VBS\_sub}) - \text{METime}(\text{Int})} \quad (5) \\
&= \frac{X_2 - 0.20 \text{ s}}{3.08 - 0.20 \text{ s}} = \frac{X_3 \text{ s}}{2.88 \text{ s}} \approx 0.5887,
\end{aligned}$$

where  $\text{METime}(\text{VBS\_fsub\_only})$  is the ME time of the subpixel refinement part of fast subpixel precision variable block-size ME, and  $\text{METime}(\text{VBS\_sub\_only})$  is the ME time of the subpixel refinement part of the original subpixel precision variable block-size ME. Here, the original subpixel refinement method means the full-position subpixel search. The ratio between these two ME times is

0.5887. Similarly, we can use this ratio to approximate the value of the ratio between  $\text{METime}(\text{No\_VBS\_Fsub\_only})$  and  $\text{METime}(\text{No\_VBS\_sub\_only})$ . Our objective is to estimate  $\text{METime}(\text{No\_VBS\_Fsub\_only})$ , which is found to be  $X_3 = 2.88 \text{ s} \times 0.5887 = 1.70 \text{ s}$ . Let us verify this result. The ME time of the subpixel refinement part of a single block-size fast subpixel ME is obtained by subtracting the time for integer ME (Int) from the ME time of a single block-size fast subpixel ME (No\_VBS\_Fsub), i.e.,  $1.94 - 0.20 = 1.74 \text{ s}$ . This value is very close to the above-estimated result (1.70 s), which confirms our measurement and the relationship between the computational complexity of our fast subpixel ME and that of the full-position subpixel ME. Hence the data in Fig. 9 can reveal, very well, the time saved for various parts of our fast strategies for ME. For example, let us say 62.88%

**Table 8** Performance comparison of ME algorithms.

Sequences		FS with VBS Integer ME and subpixel refinement	EPZS with VBS Integer ME and subpixel refinement	UMHexagonS with VBS Integer ME and subpixel refinement	No fast VBS, no SubPEL elimination, no fast SubPELME	Fast VBS, no SubPEL elimination, no fast SubPEL ME	No fast VBS, SubPEL elimination, no fast SubPEL ME	No fast VBS, no SubPEL elimination, Fast SubPEL ME	PRES
Claire	PSNR	41.75	41.72	41.66	41.67	41.57	41.67	41.70	41.67
	Bits per pixel	0.0287	0.0285	0.0287	0.0286	0.0320	0.0308	0.0291	0.0302
	Speedup (real time)	1	7	9	8	20	27	15	38
Akiyo	PSNR	39.86	39.85	39.83	39.82	39.75	39.82	39.83	39.77
	Bits per pixel	0.0307	0.0307	0.0308	0.0307	0.0344	0.0345	0.0315	0.0332
	Speedup (real time)	1	7	10	8	21	32	17	41
Mother_ daughter	PSNR	38.98	38.99	38.98	38.98	38.89	38.98	38.94	38.95
	Bits per pixel	0.0505	0.0505	0.0508	0.0508	0.0562	0.0526	0.0507	0.0515
	Speedup (real time)	1	9	13	10	25	36	16	43
Hall	PSNR	37.94	37.92	37.92	37.91	37.82	37.85	37.92	37.83
	Bits per pixel	0.0914	0.0912	0.0917	0.0920	0.1011	0.0851	0.0903	0.0809
	Speedup (real time)	1	9	13	10	26	37	21	53
Silent	PSNR	36.15	36.15	36.15	36.16	36.11	36.16	36.14	36.16
	Bits per pixel	0.0854	0.0858	0.0860	0.0866	0.1005	0.0824	0.0869	0.0800
	Speedup (real time)	1	10	13	11	30	42	20	60
Highway	PSNR	38.62	38.60	38.60	38.59	38.52	38.64	38.59	38.65
	Bits per pixel	0.0885	0.0907	0.0901	0.0915	0.1063	0.0987	0.0916	0.0983
	Speedup (real time)	1	10	12	11	29	41	17	52
Container	PSNR	36.10	36.08	36.07	36.06	35.99	36.03	36.06	36.02
	Bits per pixel	0.0703	0.0705	0.0705	0.0706	0.0751	0.0749	0.0721	0.0772
	Speedup (real time)	1	11	16	13	34	50	25	61
Erik	PSNR	37.15	37.13	37.13	37.14	37.08	37.19	37.14	37.21
	Bits per pixel	0.0759	0.0757	0.0757	0.0755	0.0843	0.0713	0.0761	0.0694
	Speedup (real time)	1	10	12	11	29	42	19	55
Paris	PSNR	35.99	35.99	35.99	35.98	35.92	35.96	35.98	35.94
	Bits per pixel	0.2054	0.2054	0.2062	0.2062	0.2484	0.1762	0.2080	0.1679
	Speedup (real time)	1	10	14	12	36	46	20	63
Foreman	PSNR	36.98	36.96	36.96	36.94	36.89	37.01	36.97	37.02

Table 8 (Continued).

Sequences	FS with VBS Integer ME and subpixel refinement	EPZS with VBS Integer ME and subpixel refinement	UMHexagonS with VBS Integer ME and subpixel refinement	No fast VBS, no SubPEL elimination, no fast SubPELME	Fast VBS, no SubPEL elimination, no fast SubPEL ME	No fast VBS, SubPEL elimination, no fast SubPEL ME	No fast VBS, no SubPEL elimination, Fast SubPEL ME	PRES	
	Bits per pixel	0.1399	0.1414	0.1412	0.1424	0.1783	0.1404	0.1443	0.1423
	Speedup (real time)	1	10	13	12	33	44	16	53
Football	PSNR	37.76	37.74	37.76	37.78	37.78	37.81	37.78	37.83
	Bits per pixel	0.2253	0.2280	0.2287	0.2323	0.2497	0.2265	0.2326	0.2262
	Speedup (real time)	1	13	14	16	42	58	20	67
Waterfall	PSNR	35.03	35.04	35.03	35.04	34.98	35.04	35.04	35.05
	Bits per pixel	0.1112	0.1118	0.1120	0.1117	0.1311	0.1158	0.1118	0.1149
	Speedup (real time)	1	13	16.41	15	38	58	20	64
Coastguard	PSNR	35.30	35.30	35.30	35.30	35.22	35.29	35.30	35.29
	Bits per pixel	0.4836	0.4840	0.4836	0.4835	0.5157	0.4693	0.4838	0.4649
	Speedup (real time)	1	15	16	18	47	67	23	76
Bus	PSNR	35.61	35.63	35.63	35.64	35.56	35.64	35.63	35.66
	Bits per pixel	0.4670	0.4651	0.4689	0.4663	0.5306	0.4526	0.4674	0.4461
	Speedup (real time)	1	14	14.63	16	45	61	22	68
Tempete	PSNR	35.47	35.46	35.45	35.46	35.37	35.45	35.46	35.43
	Bits per pixel	0.5049	0.5049	0.5050	0.5061	0.5379	0.4850	0.5096	0.4832
	Speedup (real time)	1	14	14	16	45	62	21	68
Stefan	PSNR	36.33	36.32	36.32	36.31	36.25	36.34	36.32	36.34
	Bits per pixel	0.4596	0.4606	0.4637	0.4622	0.5151	0.4411	0.4644	0.4360
	Speedup (real time)	1	13	14	15	43	55	20	63
Flower	PSNR	36.09	36.08	36.07	36.07	36.05	36.20	36.07	36.20
	Bits per pixel	0.6371	0.6376	0.6378	0.6383	0.7103	0.6045	0.6392	0.5931
	Speedup (real time)	1	12	14	14	37	51	21	63
Mobile	PSNR	35.12	35.11	35.11	35.12	34.96	35.10	35.10	35.10
	Bits per pixel	0.8199	0.8157	0.8166	0.8136	0.8699	0.7300	0.8191	0.7248
	Speedup (real time)	1	15	15	18	52	67	24	78
Averages	PSNR	37.01	37.00	37.00	37.00	36.93	37.01	37.00	37.01
	Bits per pixel	0.2542	0.2543	0.2549	0.2549	0.2820	0.2429	0.2560	0.2400
	Speedup (real time)	1	11	13	13	35	49	20	60

**Table 9** Performance comparison of ME algorithms.

Sequences	EPZS		UMHexagonS		Present algorithm	
	BDPSNR	BDBR	BDPSNR	BDBR	BDPSNR	BDBR
Carphone (QCIF)	-0.022	0.515	-0.036	0.838	0.159	-3.895
Foreman (QCIF)	0.001	-0.017	-0.026	0.689	0.006	-0.181
Salesman (QCIF)	-0.02	0.434	-0.039	0.837	0.329	-6.79
Mother_ daughter (CIF)	-0.009	0.251	-0.033	0.856	-0.212	5.573
Silent (CIF)	-0.025	0.606	-0.04	0.964	0.202	-4.942
Foreman (CIF)	-0.073	2.04	-0.07	1.939	-0.083	2.204
Football (CIF)	-0.093	1.916	-0.092	1.903	-0.01	0.234
Waterfall (CIF)	-0.014	0.405	-0.019	0.513	-0.163	4.632
Coastguard (CIF)	-0.012	0.289	-0.011	0.23	0.127	-2.951
Bus (CIF)	0.034	-0.68	-0.02	0.398	0.233	-4.674
Tempete (CIF)	-0.016	0.349	-0.028	0.62	0.108	-2.517
Stefan (CIF)	-0.018	0.416	-0.06	1.355	0.191	-4.394

of the ME time required by subpixel precision variable block-size ME is saved by using only the fast variable block-size strategy, and if we use the fast subpixel ME strategy only, then our approach can save 41.13% of the ME time.

Table 6 shows the performance comparison of full search (FS), enhanced predictive zonal search (EPZS), fast variable block-size ME algorithm in Ref. 14 (FORMER) and our fast variable block-size ME strategy (PRES). Both FS and EPZS are given by JM12.2.<sup>22</sup> All four algorithms were done without subpixel refinement at this stage. Table 6 shows the FORMER algorithm is slightly faster than EPZS, while our variable block-size strategy can achieve much faster speed than FORMER with similar PSNR and bits per pixel performance as the FS and EPZS.

Table 7 shows the performance comparison of full-position subpixel ME search, our proposed fast subpixel ME strategy, interpolation free subpixel ME,<sup>16,17</sup> and fast fractional PEL (picture element) ME.<sup>18</sup> All of them were done with fixed block size:  $16 \times 16$ . The computational complexity of interpolation free subpixel ME algorithm is similar to that of the full-position subpixel ME search, so it has less degradation on PSNR. The fast fractional PEL subpixel ME has a faster speed and a PSNR degradation of **0.05 dB**. However, it has a significant bit-rate increase of 11.63%. Among them, the present of our fast subpixel ME strategy has almost the same PSNR (**36.93 dB**) and a very slight increase in bit-rate (**0.53%**) performance as compared to the full position subpixel ME algorithm, and it has a relatively high speedup factor (i.e., **1.62** times of the full position subpixel ME speed). Table 7 shows the experimental results of the 18 sequences arranged according to the motion activities of the sequences from low to medium to high values. Again, let us explain the abbreviations used in the table, which reflect the performances of different versions of our algorithm, as follows:

“No fast VBS, no SubPEL, no fast SubPELME” means subpixel precision variable block-size ME without fast strategies. “Fast VBS, no SubPEL elimination, no fast SubPEL ME” means subpixel precision variable block-size ME with fast strategies for making mode selections (see Sec. 3.1). “No fast VBS, SubPEL elimination, no fast SubPEL ME” means subpixel precision variable block-size ME with the subpixel ME elimination method (see Sec. 3.2). “No fast VBS, no SubPEL elimination, Fast SubPEL ME” means subpixel variable block-size ME with fast strategies on subpixel ME (see Sec. 3.3). “PRES” means the present algorithm, which is the final version of our algorithm, and these results were found by making use of all three groups of our fast strategies.

The final version of our algorithm (PRES) is composed of fast variable block-size ME strategy, subpixel ME elimination strategy, and fast subpixel ME strategy. It is compared to the full-search ME algorithm and the EPZS. Both FS and EPZS are given by JM12.2.<sup>19</sup> The FS algorithm includes the VBS full search integer-pixel ME and the full-position subpixel refinement. The EPZS is composed of the fast VBS integer-pixel ME and subpixel refinement with a fast termination strategy using JM12.2. All algorithms used a SAD function for evaluation with a partial distortion search method as the basic technique.

The performance comparison includes PSNR, Bits per pixel, and Speedup (real time), where PSNR means the average PSNR values of the luminance component of the decoded frames. “Bits per pixel” gives the number of bits to code 1 pixel on average while the number of frames was set to 150 for all sequences. “Speedup (real time)” is the ratio between ME time of the FS and the ME time of the respective fast algorithms being considered. (The computational time of one algorithm for one test sequence was obtained from the average of 12 executions. After the executions, two higher values



and two lower values were deleted. Then the average value of the eight values that remain is the required computational time.)

Furthermore, Table 8 gives the performance of five versions of our algorithm. The PSNR and bits per pixel do not change much while the speedup increases from 13, 20, 35, 49, to 60 as compared to the full-search algorithm with subpixel refinement and termination strategy. This matches Fig. 9, which also shows the speedup improvement made by using our fast variable block-size strategies and fast subpixel ME strategies, respectively. Table 8 clearly shows the effect of subpixel ME elimination among various modes. A speedup of 49 is achieved by this strategy, which confirms its significance in our subpixel precision variable block-size ME scheme.

If we compare the PSNR values of the full search and EPZS of each sequence, it is not difficult to find that the PSNR values of EPZS are lower than those of the full search for 13 sequences. It has the same PSNR value with the Full Search for three sequences and higher PSNR values for two other sequences. The PSNR values of UMHexagonS are lower than that of the full search for 11 sequences, the same as that of the full search for six sequences, and higher for one sequence. However, when we compare the PSNR of the full search to the proposed algorithm, we can see that the proposed algorithm has lower PSNR values for nine sequences and the decreases vary from 0.01 to 0.11, while it has higher PSNR values for the other nine sequences and the increases also vary from 0.01 to 0.11. Hence, it is not surprising that the average PSNR of the proposed algorithm is the same as that of the full search. For bit-rate performance, all the three fast search algorithms (EPZS, UMHexagonS, our algorithm) have a similar bit-rate performance as that of the full search. Besides PSNR and bit rate, the proposed algorithm is much faster than the full search, UMHexagonS and EPZS. There is speedup of 60 times faster than the speed of full search, five times faster than the speed of EPZS, and four times faster than the speed of UMHexagonS. The speedup value varies from 38 to 78 as compared to the full search. If the motion in a sequence is mainly translational, then the speedup ratio is usually high, even without degradation or a decrease in PSNR. This is the situation for the bus sequence, for example, as shown in Table 8.

The proposed algorithm is also efficient for using other QP values. Table 9 gives the performance comparison among FS, UMHexagonS, EPZS, and the proposed ME algorithm using different QP values. Each entry in Table 9 was obtained from 12 sequences (three sequences with the format  $176 \times 144$  and nine sequences with the format  $352 \times 288$ ). From Table 9, we can see that the proposed algorithm can always achieve very similar PSNR and bits-per-pixel performance compared to the FS. It has a noticeably higher speedup value than that of the EPZS (or UMHexagonS) as shown in Table 8. For a high-QP condition, the speedup value decreases slightly (for example, the speedup value changes from 54 to 46 for varying the QP from 30 to 38, respectively). The reason for this is that the image distortion may become serious with a high-QP condition. The acceleration strategies based on our analysis of the motion characteristics of successive frames are affected by the image distortion. This is a compromise that we have to pay for a guarantee of the video quality of the encoded sequence.

**Table 10** Performance comparison of different algorithms, VM: JM12.2.

Sequences		FS	EPZS	PRES
CrowdRun	PSNR	35.63	35.63	35.61
	Bits per pixel	0.4574	0.4575	0.3731
	Speedup (real time)	1	9	52
ParkJoy	PSNR	35.59	35.59	35.64
	Bits per pixel	0.6839	0.6842	0.5994
	Speedup (real time)	1	10	61
DucksTakeOff	PSNR	35.23	35.24	35.23
	Bits per pixel	0.7936	0.7963	0.7504
	Speedup (real time)	1	10	69
InToTree	PSNR	35.07	35.04	35.04
	Bits per pixel	0.0645	0.0666	0.0754
	Speedup (real time)	1	10	50
OldTownCross	PSNR	35.34	35.33	35.30
	Bits per pixel	0.0622	0.0623	0.0672
	Speedup (real time)	1	10	45
Average	PSNR	35.37	35.37	35.36
	Bits per pixel	0.4123	0.4134	0.3731
	Speedup (real time)	1	10	56

We have also made an evaluation of our algorithm using some high-definition video sequences as shown in Table 10. Five sequences with a resolution of  $1920 \times 1080$  were tested. These include CrowdRun and ParkJoy sequences, which are two motion-intensive sequences; DucksTakeOff sequence, which has irregular water wave motion; and InToTree and OldTownCross sequences, which contain both zoom and translation motion activities. All these sequences contain plenty of image details. Results of this experimental work show that our algorithm has nearly the same PSNR as the FS, and the bit-rate performance is also very similar. However, the speedup ratio of our algorithm compared to the FS is 56, which is substantially higher than the speedup value of EPZS. This speed performance is similar to that achieved in lower resolution video sequences.

In some of our experimental results, the performance of the present approach appears, in terms of both PSNR quality and bit rate, better than the full search. It is due to the inaccuracy of the RD evaluation of the JM software, which cannot optimize all factors simultaneously. In principle, the evaluation should give us the best trade-off among motion-vector size, residual signal, intra- and intermode selection, mode-type selection, etc. Actually, the optimization can be done, generally, but not too ideally, and this is a very good topic

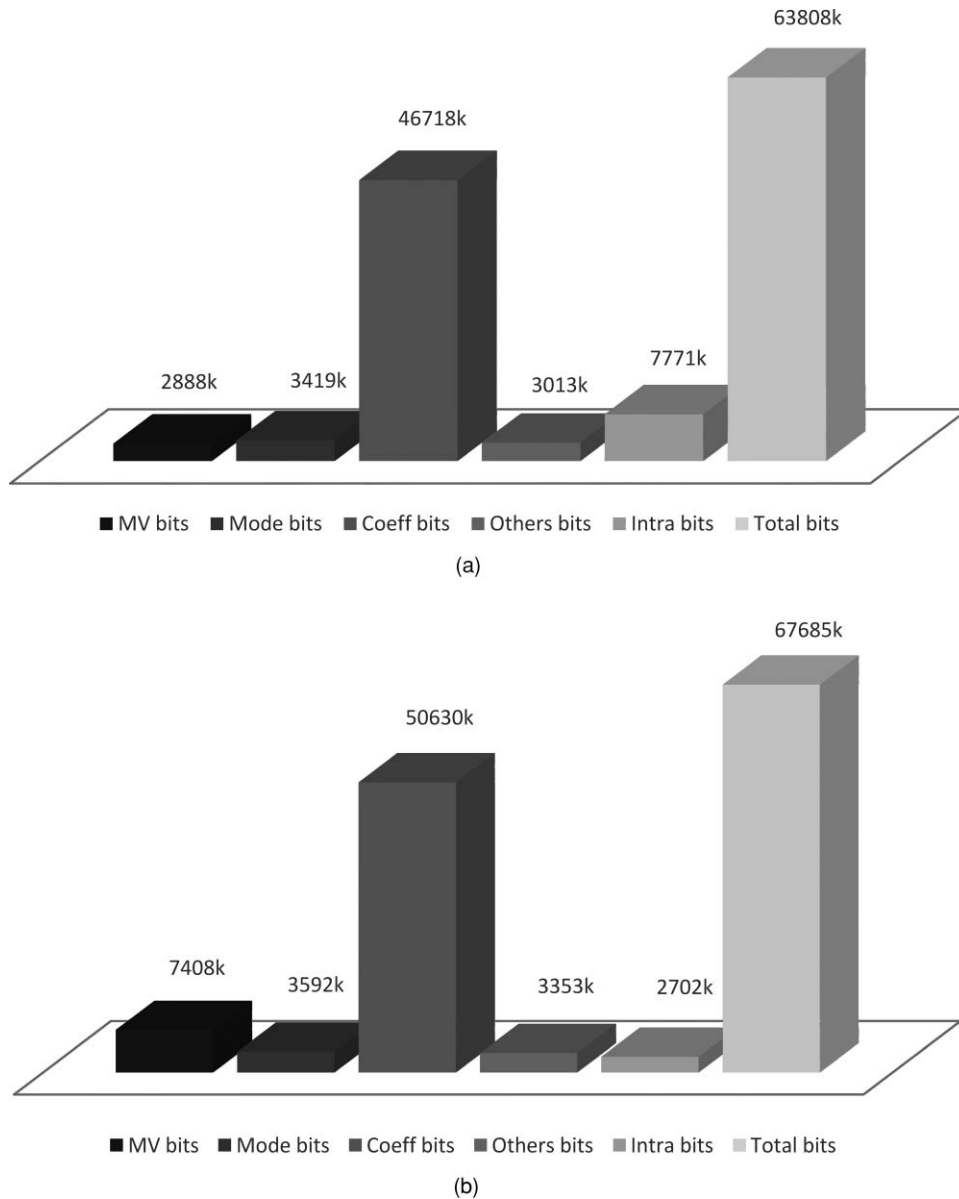


Fig. 10 Bits distribution of (a) PRES and (b) FS.

deserving for much further research in the future. Figure 10 shows the accumulated bits distribution of 18 standard test sequences using the present approach (PRES) or FS ME algorithms with QP equal to 28. The FS working under the rate distortion (RD) evaluation can automatically acquire shorter motion vectors, but more “Intra bits” are required, for example. This also results in that more “Coeff bits” of the FS being required as compared to that of PRES. Hence, the “Total bits” of PRES is lower than FS. This is just an example to explain the reason that PRES can achieve lower bits per pixel when the QP is >32, as shown in Table 9.

## 5 Conclusion

In many cases, there are two main reasons for making a fast ME algorithm be less efficient; namely, some promising locations may be skipped or some unnecessary searches may be continued. In the latter case, we may not even be aware

that there are many unnecessary time-consuming steps in the algorithm. Each of these two types of problems will generate a certain degradation of the image quality, and the unnecessary searching will affect the efficiency. However, these are apparently two conflicting points. Usually, a smart trade-off between these two points must be achieved, or a better solution is to prevent both cases from happening. This in turn relies on a critical and yet simple analysis of the current data to make decisions for the fast algorithm. We have successfully resolved these problems by formulating our fast strategies based on the motion information of blocks in the previous frame and on their current statistics. The fast strategies are based on particular properties even at the individual block level.

We have done an analysis of the statistics of the mode selection of variable block-size ME. We found that >80% of the computation does not provide a better result in the original algorithm given by JM12.2, for example. We have also

done much work to analyze the relationship of the ME results of different block sizes, the relationship between mode decision and subpixel ME, the relationship among candidate checking points of half-pixel ME, and the relationship between half-pixel and quarter-pixel ME results. The analysis reveals the possibility of making early termination and early mode decisions with little damage to the search results. It also reflects the principle of fast strategies and may give clues on how fast strategies be used.

The proposed new method for making early terminations and early mode selections of variable block size ME relies heavily on the motion information from all blocks and their statistical information of the successive frames. The statistical information can adaptively be updated to fit the new incoming frames. We have to make some presumptions based on the motion information and the statistics information. These conditional presumptions are very close to the real situations. Even though there are few occasional misses of the best match or misses of the best mode with our fast strategies, we have found that the degradation of image quality is not substantial at all. Results of our experimental work also show that our approach can be over four times faster than the algorithms available in the reference software of H.264 (JM12.2). Even though we have found that our algorithm is better than other algorithms available in the literature, there is still plenty of room for improvement. We may make an exploitation in a more systematic way to find out more immediate information to help us make the correct decision. We may compare the actual situation with the correctness of our decision rules. What is the percentage of decisions that are successful? How far can we trim our algorithm with >95% correct decisions yet still have an overall improvement of the new algorithm? This is a fruitful direction for further research.

### Acknowledgment

This research work is supported in part by the Centre for Signal Processing (1BB87) of the Hong Kong Polytechnic University, CERG grant (B-Q07G) of the Hong Kong SAR Government and the Beijing Institute of Technology.

### References

1. Y.-L. Chan and W.-C. Siu, "An efficient search strategy for block motion estimation using image features," *IEEE Trans. Image Process.* **10**(8), 1223–1238 (August 2001).
2. K.-C. Hui, W.-C. Siu, and Y.-L. Chan, "New adaptive partial distortion search using clustered pixel matching error characteristic," *IEEE Trans. Image Process.* **14**(5), 597–607 (May 2005).
3. A. M. Tourapis, O. C. Au, M. L. Liou, and G. Shen, "Fast and efficient motion estimation using diamond zonal based algorithms," *J. Circuits Syst. Signal Process.* **20**(2), 233–251 (June 2001).
4. Y.-L. Chan and W.-C. Siu, "New adaptive pixel decimation for block motion vector estimation," *IEEE Trans. Circuits Syst. Video Technol.* **6**(1), 113–118, (February 1996).
5. P. I. Hosur and K.-K. Ma, "Motion vector field adaptive fast motion estimation," presented at 2nd Int. Conf. on Information, Communications and Signal Processing (ICIS'99), (December 1999).
6. I. Ahmad, W. Zheng, L. Jiancong, and L. Ming, "A fast adaptive motion estimation algorithm," *IEEE Trans. Circuits Syst. Video Technol.* **16**(3), 420–438 (March 2006).
7. Y. Zhang, W.-C. Siu, and T. Shen, "Yet a faster motion estimation algorithm with directional search strategies," *Proc. of 15th IEEE Int. Conf. on Digital Signal Processing*, Cardiff, UK, pp. 475–478 (July 2007).
8. Y. Zhang and T. Shen, "Motion information based adaptive block classification for fast motion estimation," *Proc. of IEEE Int. Conf. Neural Networks and Signal Processing*, Zhenjiang, China, pp. 686–691 (June 2008).
9. K.-C. Hui and W.-C. Siu, "Extended analysis of motion-compensated frame difference for block-based motion prediction error," *IEEE Trans. Image Process.* **16**(5), 1232–1245 (May 2007).
10. Liangming Ji and Wan-Chi Siu, "Reduced computation using adaptive search window size for H.264 Multi-Frame Motion Estimation," *Proc. of 14th Eur. Signal Processing Conf. (EUSIPCO'2006)*, Florence, Italy, IEEE Paper No. 1568982117 (September 2006).
11. L. Yang, K. Yu, J. Li, and S. Li, "An effective variable block-size early termination algorithm for H.264 video coding," *IEEE Trans. Circuits Syst. Video Technol.* **15**(6), 784–788 (June 2005).
12. S. Saponara, M. Casula, F. Rovati, D. Alfonso, and L. Fanucci, "Dynamic control of motion estimation search parameters for low complex H.264 Video Coding," *IEEE Trans. Consumer Electron.* **52**(1), 232–239 (February 2006).
13. Y.-W. Huang, B.-Y. Hsieh, S.-Y. Chien, S.-Y. Ma, and L.-G. Chen, "Analysis and complexity reduction of multiple reference frames motion estimation in H.264 AVC," *IEEE Trans. Circuits Syst. Video Technol.* **16**(4), 507–522 (April 2006).
14. C. Grecos and M. Y. Yang, "Fast inter mode prediction for P slices in the H264 Video Coding Standard," *IEEE Trans. Broadcast.* **51**(2), 256–263 (June 2005).
15. T.-Y. Kuo and C.-H. Chan, "Fast variable block size motion estimation for H.264 using likelihood and correlation of motion field," *IEEE Trans. Circuits Syst. Video Technol.* **16**(10), 1185–1195 (October 2006).
16. J. Lee and B. Jeon, "Fast mode decision for H.264 with variable motion block sizes," *Lect. Notes Comput. Sci.* **2869**, 723–730 (2003).
17. P. R. Hill, T. K. Chiew, D. R. Bull, and C. N. Canagarajah, "Interpolation free subpixel accuracy motion estimation," *IEEE Trans. Circuits Syst. Video Technol.* **16**(12), 11519–11526 (December 2006).
18. J. W. Suh and J. Jeong, "Fast sub-pixel motion estimation techniques having lower computational complexity," *IEEE Trans. Consumer Electron.* **50**(3), 968–973 (August 2004).
19. Y.-J. Wang, C.-C. Cheng, and T.-S. Chang, "A fast fractional PEL motion estimation algorithm for H.264/MPEG-4 AVC," *Proc. IEEE Int. Sym. Circuits and Systems (ISCAS)*, Island of Kos, Greece, pp. 3974–3977 (May 2006).
20. W. Lin, D. Baylon, K. Panusopone, and M.-T. Sun, "Fast sub-pixel motion estimation and mode decision for H.264," in *Proc. of IEEE Int. Symp. on Circuits and Systems (ISCAS)*, Washington, pp. 3482–3485 (May 2008).
21. L. Yang, K. Yu, J. Li, and S. Li, "Prediction-based directional fractional pixel motion estimation for H.264 video coding," in *Proc. of IEEE Int. Conf. on Acoustics, Speech, and Signal Processing*, Philadelphia, pp. 901–904 (March 2005).
22. Joint Video Team (JVT) of ISO/IEC MPEG & ITU-T VCEG, "Draft ITU-T Recommendation and Final Draft International Standard of Joint Video Specification (ITU-T Rec. H.264| ISO/IEC 14496-10 AVC)," JVT-G050 (March 2003).



**Ying Zhang** received the BE and PhD degrees in Electronic Engineering from Beijing Institute of Technology, China, in 2004 and 2009, respectively. Dr. Zhang was a visiting student at Hong Kong Polytechnic University from 2006 to 2008. Since 2009, she has been with the Digital Media Center at Vimicro Company Ltd., where she is a research engineer. Her research interests include image and video coding, video signal processing, architecture of video codec and multimedia system design.



**Wan-Chi Siu** received his MPhil and PhD degrees from CUHK and Imperial College, UK, in 1977 and 1984 respectively. He joined the Hong Kong Polytechnic University in 1980, and was head of Electronic and Information Engineering Department and subsequently Dean of Engineering Faculty between 1994 and 2002. He has been chair professor since 1992 and is now director of the Centre for Signal Processing. He is an expert in DSP, specializing in fast algorithms, video coding, transcoding, 3-D videos and pattern recognition, and has published 380 research papers, over 160 of which appeared in international journals, such as *IEEE Transactions on Image Processing*. He has been guest editor/associate editors of many journals, and keynote speaker and chief organizer of many important conferences. His work on fast computational algorithms (such as DCT) and motion

estimation algorithms have been well received by academic peers, with good citation records, and a number of which are now being used in hi-tech industrial applications, such as modern video surveillance and video codec design for HDTV systems.



**Tingzhi Shen** received BS from the Beijing Institute of Technology in 1967. She is now a professor in the Department of Electronic Engineering, Beijing Institute of Technology. She is a member of the Chinese Institute of Electronics, an expert of the Scientific Research Foundation for the Returned Overseas Chinese Scholars State Education Ministry and a member of Self-study Examination Group of State Education Ministry.

She visited the UMASS Digital Image Analysis Center of America as a visiting researcher in 1986 and 1994, and visited the University of Lancashire in 1993. She has been very successful in research fund applications, and able to secure various research projects from the National Science Foundation, National Defense Pre-Research Foundation, and Institute of Electric Power Foundation. She has received awards from the university for her research work and publication contributions. She has published over 20 research papers. Her research interests include image processing and pattern recognition.